

International Journal of Modern Physics A
 © World Scientific Publishing Company

Implications of the first AMS-02 antiproton data for dark matter

Hong-Bo Jin^{a,b}, Yue-Liang Wu^{a,c,d}, and Yu-Feng Zhou^{a,c}

^{a)} *State Key Laboratory of Theoretical Physics,* ^{b)} *National
Astronomical Observatories, Chinese Academy of Sciences,*

^{c)} *Kavli Institute for Theoretical Physics China, Institute of
Theoretical Physics Chinese Academy of Sciences,*

^{d)} *University of Chinese Academy of Sciences,
Beijing, 100190, P.R. China*

The implications of the first AMS-02 \bar{p}/p data for the propagation of cosmic rays and the properties of dark matter (DM) are discussed. Using various diffusive re-acceleration (DR) propagation models, one can derive very conservative upper limits on the DM annihilation cross sections. The limits turned out to be compatible with that from the Fermi-LAT gamma-ray data on the dwarf spheroidal satellite galaxies. The flattening of the \bar{p}/p spectrum above ~ 100 GeV in the current data still leaves some room for TeV scale DM particles. More antiproton data at high kinetic energies are needed to constrain the properties of the DM particles.

Cosmic-ray antiparticles, such as positrons and antiprotons play important roles in the indirect search for dark matter (DM) in the Galactic halo. The Alpha Magnetic Spectrometer (AMS-02) is measuring such cosmic-ray charged particles with unprecedented accuracies. So far the anomalous rise in the positron fraction previously reported by PAMELA^{1,2} and Fermi-LAT³ has been confirmed by AMS-02 with higher accuracy and extended to higher energies,⁴ which has triggered extensive theoretical studies on possible explanations including halo DM annihilation or decay (for recent global analyses on AMS-02 data, see e.g. Refs^{5–15}). Antiprotons are highly expected from DM annihilation in many DM models, which is unlikely to be generated from the nearby pulsars.

Recently, the AMS-02 collaboration has released the first preliminary result of the cosmic-ray antiproton to proton flux ratio \bar{p}/p .¹⁶ The measured kinetic energies of the antiprotons have been extended to ~ 450 GeV. Although the spectrum of \bar{p}/p at high energies above 100 GeV tend to be relatively flat, within uncertainties the AMS-02 data are consistent with the background of secondary antiprotons, which can be used to set stringent upper limits on the dark matter (DM) annihilation cross sections, especially for high mass DM particles. The constraints on the DM properties from antiprotons have been investigated previously before AMS-02 (see e.g.^{17–21}). In this talk, we briefly summarise our work on the implications of the new AMS-02 \bar{p}/p data for constraining the annihilation cross sections of the DM particles in various propagation models and DM profiles. The details of the analysis can be found in Ref.²²

In the diffusion models of cosmic-ray propagation, the Galactic halo within which the diffusion processes occur is parametrized by a cylinder with radius $R_h = 20 - 30$ kpc and half-height $Z_h = 1 - 20$ kpc. The diffusion equation for the cosmic-ray charged particles reads

$$\begin{aligned} \frac{\partial \psi}{\partial t} = & \nabla(D_{xx}\nabla\psi - \mathbf{V}_c\psi) + \frac{\partial}{\partial p}p^2D_{pp}\frac{\partial}{\partial p}\frac{1}{p^2}\psi - \frac{\partial}{\partial p}\left[\dot{p}\psi - \frac{p}{3}(\nabla \cdot \mathbf{V}_c)\psi\right] \\ & - \frac{1}{\tau_f}\psi - \frac{1}{\tau_r}\psi + q(\mathbf{r}, p), \end{aligned} \quad (1)$$

where $\psi(\mathbf{r}, p, t)$ is the number density per unit of total particle momentum. For steady-state diffusion, it is assumed that $\partial\psi/\partial t = 0$. The number densities of cosmic-ray particles are assumed to be vanishing at the boundary of the halo. The energy dependent spatial diffusion coefficient D_{xx} is parametrized as $D_{xx} = \beta D_0 (\rho/\rho_0)^\delta$, where ρ is the rigidity of the cosmic-ray particle. The power spectral index δ can have different values $\delta = \delta_{1(2)}$ for ρ below (above) a reference rigidity ρ_0 . D_0 is a normalization constant. The convection term in the diffusion equation is related to the drift of cosmic-ray particles from the Galactic disc due to the Galactic wind. The diffusion in momentum space is described by the reacceleration parameter D_{pp} which is related to the Alfvén speed V_a of disturbances in the hydrodynamical plasma.²³ The momentum loss rate is denoted by \dot{p} , and $\tau_f(\tau_r)$ is the time scale for fragmentation (radioactive decay) of the cosmic-ray nuclei.

The spectrum of a primary source term for a cosmic-ray nucleus A is assumed to have a broken power law behaviour $dq_A(p)/dp \propto (\rho/\rho_{As})^{\gamma_A}$ with $\gamma_A = \gamma_{A1}(\gamma_{A2})$ for the nucleus rigidity ρ below (above) a reference rigidity ρ_{As} . The spatial distribution of the primary sources is assumed to follow that of the pulsars and is taken from Ref.²⁴ The background antiproton is assumed to only have the secondary origin, namely, they are created dominantly from inelastic pp - and pA -collisions with the interstellar gas. The corresponding source term reads

$$q_{\text{sec}}(p) = \beta c n_i \sum_{i=\text{H,He}} \int dp' \frac{\sigma_i(p, p')}{dp'} n_p(p'), \quad (2)$$

where n_i is the number density of the interstellar hydrogen (helium), n_p is the number density of primary cosmic-ray proton per total momentum, and $d\sigma_i(p, p')/dp'$ is the differential cross section for $p + \text{H(He)} \rightarrow \bar{p} + X$. In calculating the antiprotons, inelastic scattering to produce “tertiary” antiprotons should be taken into account. The primary source from the annihilation of Majorana DM particles has the following form

$$q_{\text{DM}}(\mathbf{r}, p) = \frac{\rho(\mathbf{r})^2}{2m_\chi^2} \langle \sigma v \rangle \sum_X \eta_X \frac{dN^{(X)}}{dp}, \quad (3)$$

where $\langle \sigma v \rangle$ is the velocity-averaged DM annihilation cross section multiplied by DM relative velocity. $\rho(\mathbf{r})$ is the DM energy density distribution function, and $dN^{(X)}/dp$ is the injection energy spectrum of antiprotons from DM annihilating into SM final states through possible intermediate states X with η_X the corresponding branching fractions. The interstellar flux of the cosmic-ray particle is related to its density function as $\Phi = v\psi(\mathbf{r}, p)/(4\pi)$. At the top of the atmosphere (TOA) of the Earth, the fluxes of cosmic-rays are affected by solar winds and the heliospheric magnetic field. This effect is taken into account using the force-field approximation which involves the Fisk potential ϕ .²⁵ We shall take $\phi = 550$ MV in numerical analysis.

We solve the diffusion equation of Eq. (1) using the publicly available code GALPROP v54^{26–30} which utilizes realistic astronomical information on the distribution of interstellar gas and other data as input, and considers various kinds of observables in a self-consistent way. We start with the so-called “conventional” diffusive re-acceleration (DR) model^{28,30} which is commonly adopted by the current experimental collaborations as a benchmark model for the astrophysical backgrounds. It is useful to consider this model as a reference model to understand how the DM properties could be constrained by the AMS-02 data. Then we consider three representative propagation models selected from a large sample of models obtained from a global Bayesian MCMC fit to the preliminary AMS-02 proton and B/C data using the GALPROP code.³¹ They are selected to represent the typically minimal (MIN), median (MED) and maximal (MAX) antiproton fluxes within 95% CL, corresponding to the region enveloping 95% of the MCMC samples with highest likelihoods in a six-dimensional parameter space. Note that the GALPROP based “MIN”, “MED”

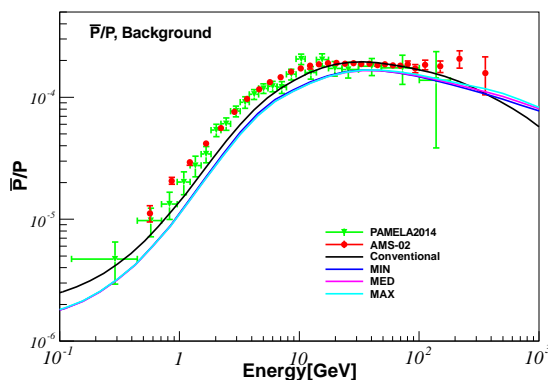


FIG. 1. Predictions for the \bar{p}/p ratio from the four propagation models. The data from AMS-02¹⁶ and PAMELA³⁶ are shown. See text for detailed discription.

and “MAX” models used in this work are different from and complementary to that given in Ref.³²

The predictions for the background of the \bar{p}/p flux ratio in these models are shown in Fig. 1. The “MIN”, “MED” and “MAX” models are highly degenerate in the background \bar{p}/p ratio. Compared with these models, the “conventional” model predicts more low energy antiprotons but at high energies above ~ 500 GeV, the predicted antiprotons are much less. In all the four DR propagation models, below ~ 10 GeV the GALPROP based calculations underpredict the \bar{p}/p flux ratio by $\sim 40\%$, which is a known issue. The agreement with the low energy \bar{p} data can be improved by introducing breaks in diffusion coefficients,³³ “fresh” nuclei component³⁴ or a DM contribution.¹⁷ The predictions for low energy \bar{p}/p ratio can also be easily modified by introducing an independent Fisk potential ϕ for \bar{p} and an energy-dependent overall normalization factor as discussed in Ref.³⁵ We instead use these DR models to derived very conservative upper limits on the annihilation cross sections of light DM particles. Note, however, that in the DR propagation models, the background predictions agree with the AMS-02 data well at higher energies $\sim 10 - 100$ GeV, which can be turned into stringent constraints on the nature of heavy DM particles.

We consider three reference DM annihilation channels $\bar{\chi}\chi \rightarrow XX$ where $XX = q\bar{q}$, $b\bar{b}$ and W^+W^- . The energy spectra of these channels are similar at high energies. The main difference is in the average number of total antiprotons N_X per DM annihilation of each channel. The injection spectra $dN^{(X)}/dp$ from DM annihilation are calculated using the numerical package PYTHIA v8.175.³⁷

We shall first derive upper limits on DM annihilation cross section as a function of DM particle mass, using the frequentist χ^2 -analyses. All of the 30 data points of the AMS-02 \bar{p}/p data are included in calculating the limits. In Fig. 2, we show the obtained upper limits on the cross sections for DM particle annihilation into

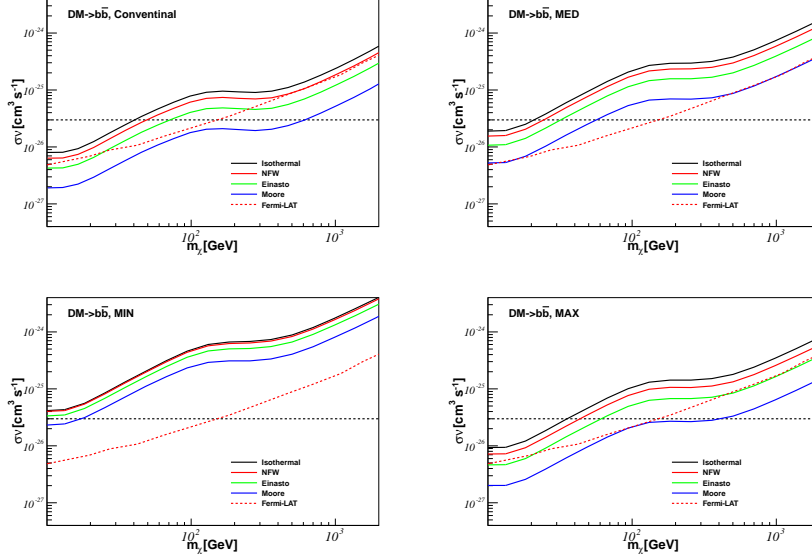


FIG. 2. Upper limits on the cross sections for DM particle annihilation into $b\bar{b}$ final states from the AMS-02 \bar{p}/p data in the “conventional” (upper left), “MED” (upper right), “MIN” (lower left) and “MAX” (lower right) propagation models. Four DM profiles NFW,³⁸ Isothermal³⁹, Einasto⁴⁰ and Moore^{41,42} are considered. The upper limits from the Fermi-LAT 6-year gamma-ray data of the dwarf spheroidal satellite galaxies of the Milky Way are also shown.⁴³ The horizontal line indicates the typical thermal annihilation cross section $\langle\sigma v\rangle = 3 \times 10^{-26} \text{cm}^3 \text{s}^{-1}$.

$b\bar{b}$ final states from the AMS-02 \bar{p}/p data in the “conventional”, “MED”, “MIN” and “MAX” propagation models. Four different DM profiles: NFW,³⁸ Isothermal,³⁹ Einasto⁴⁰ and Moore^{41,42} are considered. As can be seen, the upper limits as a function of m_χ show some smooth structure for all the final states and DM profiles. The limits tend to be relatively stronger at $m_\chi \approx 300$ GeV, which is related to the fact that the background predictions agree with the data well at the antiproton energy range $\sim 20 - 100$ GeV. For a comparison, the upper limits from the Fermi-LAT 6-year gamma-ray data of the dwarf spheroidal satellite galaxies of the Milky Way⁴³ are also shown in Fig. 2. In the “conventional” model, the upper limits from the AMS-02 \bar{p}/p data are found to be compatible with that derived from the Fermi-LAT gamma-ray data for $m_\chi \gtrsim 300$ GeV. This observation holds for most of the DM profiles. In the “MED” model, the constraints are relatively weaker, which is related to the under prediction of low energy antiprotons in this model and the limits are more conservative. For an estimation of the uncertainties due to the propagation models, from the “MIN” model to the “MAX” model, we find that the variation of the upper limits is within about a factor of five.

For the W^+W^- final states, the resulting limits are shown in Fig. 3. In the “conventional” propagation model, the constraints from AMS-02 \bar{p}/p data turn out

6 Hong-Bo Jin, Yue-Liang Wu and Yu-Feng Zhou

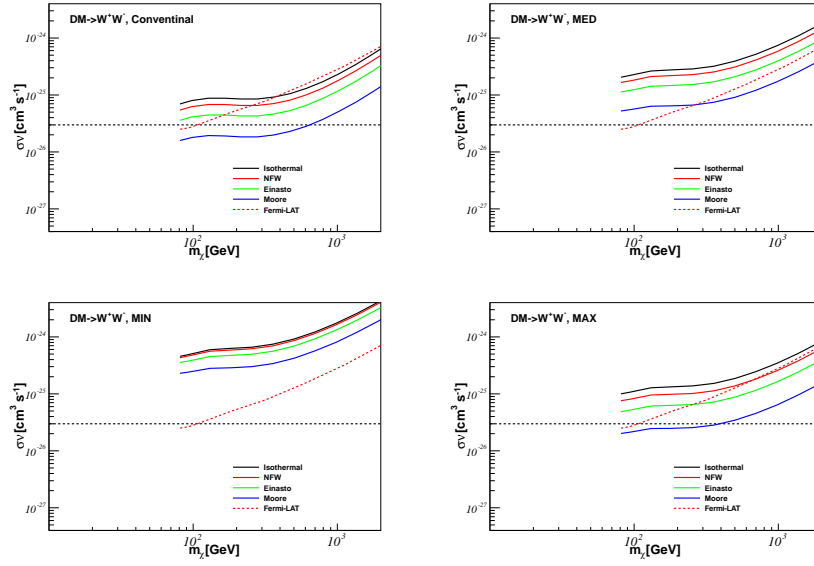


FIG. 3. The same as Fig. 2, but for DM annihilation into W^+W^- final states.

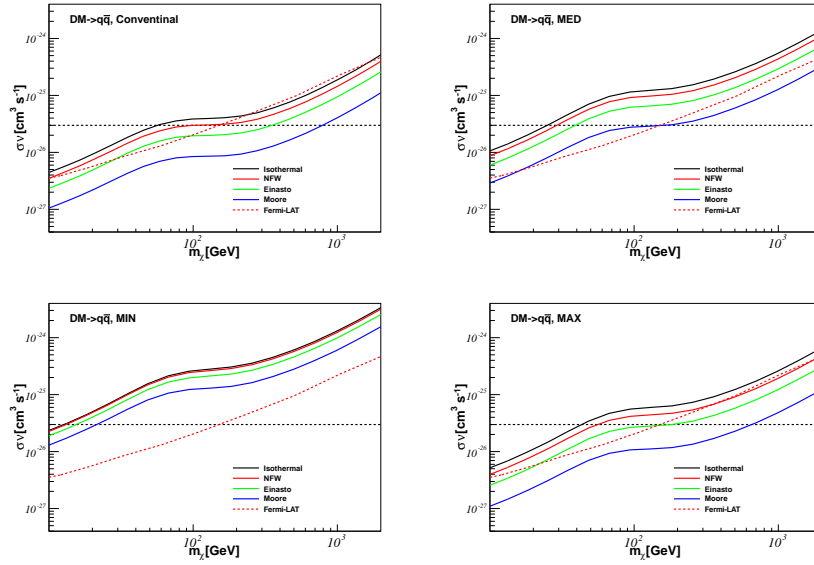


FIG. 4. The same as Fig. 2, but for DM annihilation into $q\bar{q}$ final states.

to be more stringent than that from the Fermi-LAT gamma-ray data for all the four DM profiles when the DM particle mass is above ~ 300 GeV. Again we find that the variation of the upper limits from the “MIN” to the “MAX” model is within a factor of five. The result for the $q\bar{q}$ final states is shown in Fig. 4. Compared with the case of W^+W^- and $b\bar{b}$, the constraints on the $q\bar{q}$ final states are the most stringent. For all the three final states, we find that the allowed DM annihilation cross section is below the typical thermal cross section for $m_\chi \lesssim 300$ GeV in the conventional propagation model with Einasto profile.

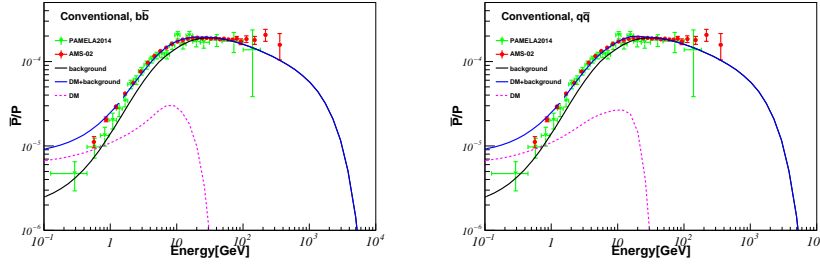


FIG. 5. Left) Spectrum of \bar{p}/p flux ratio from DM annihilating into $b\bar{b}$ final states with $m_\chi = 58.5$ GeV and $\langle\sigma v\rangle = 2.16 \times 10^{-26} \text{ cm}^3\text{s}^{-1}$ obtained from a fit to the whole AMS-02 \bar{p}/p data.¹⁶ The “conventional” background model and the Einasto DM profile are assumed. Right) The same as left, but for the fit with $q\bar{q}$ final state with the best-fit values $m_\chi = 35$ GeV and $\langle\sigma v\rangle = 0.86 \times 10^{-26} \text{ cm}^3\text{s}^{-1}$.

As shown in Fig. 1, compared with the AMS-02 data the GALPROP DR models predict fewer antiprotons at low ($\lesssim 10$ GeV) and very high ($\gtrsim 100$ GeV) energies. Without a robust estimation of the theoretical uncertainties, it is too early to claim any excesses in the \bar{p}/p data. We nevertheless consider what would be the implications for DM if such a trend in the observations is confirmed by future analyses. The low energy data would allow for a non-vanishing DM annihilation cross section. For instance, in the “conventional” propagation model, for $m_\chi = 10.1$, 35.0 and 75.8 GeV, the best-fit values are $\langle\sigma v\rangle = 3.6 \times 10^{-27}$, 1.14×10^{-26} , and $2.79 \times 10^{-26} \text{ cm}^3\text{s}^{-1}$, respectively, if the DM profile is Einasto, and the DM particles annihilate dominantly into $b\bar{b}$ final states. If both m_χ and $\langle\sigma v\rangle$ are allowed to vary freely, the best-fit DM particle masses and annihilation cross sections are $m_\chi = 58.5$ (35.0) GeV and $\langle\sigma v\rangle = 2.16$ (0.86) $\times 10^{-26} \text{ cm}^3\text{s}^{-1}$ for DM annihilating into $b\bar{b}$ ($q\bar{q}$) final states. In Fig. 5, we show the calculated spectra of \bar{p}/p flux ratio from the best-fit DM particle masses and cross sections. The figure shows that the low energy \bar{p}/p data are well reproduced by including such a DM contribution, except for the data point with kinetic energy below 1 GeV.

As shown in Fig. 1, the spectrum of the AMS-02 \bar{p}/p ratio tends to be flat toward high energies above ~ 100 GeV. This trend, if confirmed by the future AMS-02 data, is not expected from the secondary production of antiprotons, and raises the

8 Hong-Bo Jin, Yue-Liang Wu and Yu-Feng Zhou

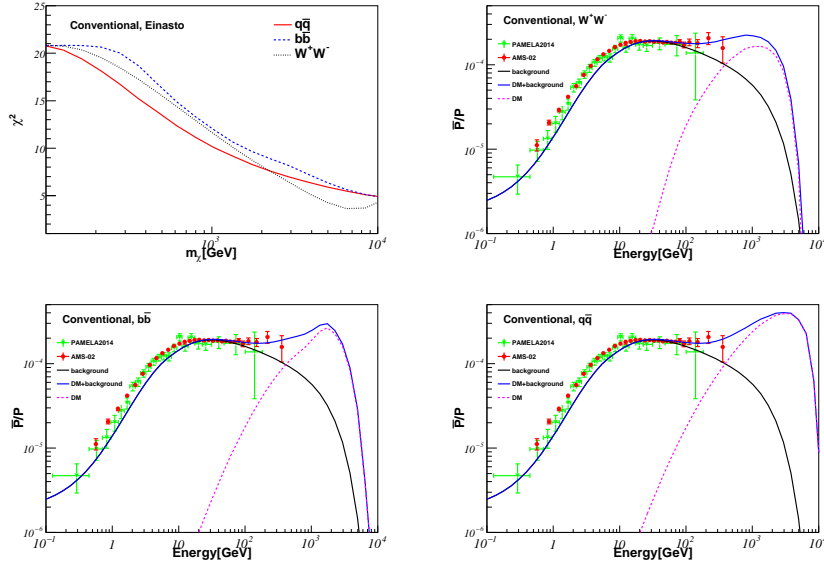


FIG. 6. (Upper left) values of χ^2_{\min} as a function of DM particle mass m_χ from a fit to the AMS-02 \bar{p}/p data (with kinetic energy above 20 GeV) in the “conventional” propagation model^{28,30} with the DM profile fixed to Einasto.⁴⁰ Three annihilation channels $b\bar{b}$, $q\bar{q}$ and W^+W^- are considered. (Upper right) predicted \bar{p}/p ratio in the case of background (“conventional” model) plus a DM contribution with $m_\chi = 6.5$ TeV, $\langle\sigma v\rangle = 1.9 \times 10^{-24} \text{ cm}^3 \text{ s}^{-1}$, and annihilation final states W^+W^- . The flux ratio of antiproton from DM to the proton from the background $\bar{p}_{\text{DM}}/p_{\text{BG}}$ is shown as the dashed line. The data from AMS-02¹⁶ and PAMELA³⁶ are also shown. (Lower left) the same as the upper right, but for the $b\bar{b}$ channel with $m_\chi = 10.9$ TeV and $\langle\sigma v\rangle = 3.4 \times 10^{-24} \text{ cm}^3 \text{ s}^{-1}$. (Lower right) the same as the upper right, but for the $q\bar{q}$ channel with $m_\chi = 10.9$ TeV and $\langle\sigma v\rangle = 3.3 \times 10^{-24} \text{ cm}^3 \text{ s}^{-1}$.

interesting question whether this would leave some room for a heavy DM contribution, similar to the case of the AMS-02 positron fraction.^{4,5,9–11} To explore this possibility, we perform an other fit using the \bar{p}/p ratio data above 20 GeV (including 15 data points in total) in order to avoid the theoretical uncertainties in the low energy region. The obtained χ^2_{\min} as a function of m_χ for the $b\bar{b}$, $q\bar{q}$ and W^+W^- final states in the “conventional” propagation model with Einasto DM profile are shown in Fig. 6. For the three final states the values of χ^2_{\min} decrease almost monotonically from ~ 21 to ~ 5 with an increasing DM particles mass from 100 GeV to 10 TeV, but the χ^2 -curves become gradually flat toward high DM masses. Only for the W^+W^- channel, there exists a shallow local minimal at around 6.5 TeV with low statistical significance. From the χ^2 -curves, one can see that the DM particles mass is restricted to be above ~ 2 TeV at 2σ . For an illustration purpose, we show in Fig. 6 the predictions for the \bar{p}/p ratio in the “conventional” background model with a DM contribution. The DM particles masses and annihilation cross sections chosen to be $m_\chi = 6.5$ TeV, $\langle\sigma v\rangle = 1.9 \times 10^{-24} \text{ cm}^3 \text{ s}^{-1}$ for W^+W^- ,

$m_\chi = 10.9$ TeV, $\langle\sigma v\rangle = 3.4 \times 10^{-24}$ cm³s⁻¹ for $b\bar{b}$ channel, and $m_\chi = 10.9$ TeV and $\langle\sigma v\rangle = 3.3 \times 10^{-24}$ cm³s⁻¹ for $q\bar{q}$ channel. Note that these values are not from the best-fit values. We conclude that introducing a DM contribution can improve the agreement with the AMS-02 \bar{p}/p data with kinetic energy above 100 GeV, but the statistics is not high enough to determine the DM properties such as its mass and interaction strength. As can be seen in Fig. 1, the possible “excess” is located at the kinetic energy range 100 – 450 GeV where the secondary backgrounds from the four propagation models are similar. However, beyond ~ 450 GeV, the \bar{p}/p from the “conventional” model drops quicker than that in the other propagation models. The future high energy antiproton data will be very important not only in probing DM but also in constraining the background models.

In conclusion, we have explored the implications of the first AMS-02 \bar{p}/p data on constraining the annihilation cross sections of the DM particles in various propagation models and DM profiles. We have derived the upper limits using the GALPROP code and shown that in the “conventional” propagation model with Einasto DM profile, the constraints can be more stringent than that derived from the Fermi-LAT gamma-ray data on the dwarf spheroidal satellite galaxies. Making use of the typical minimal, median and maximal models obtained from a previous global fit, we have shown that the uncertainties on the upper limits is around a factor of five. The future more precise AMS-02 data can help to reduce the uncertainties in the derived upper limits. The analysis in this work has some overlap with that in³⁵. Note that although the conclusions are similar, the analysis in this work is based on the fully numerical GALPROP code, while that in³⁵ is based on the two-zone diffusion model with (semi)-analytical approach. Similar discussions on the DM matter contributions can be found in Refs.^{44,45}

This work is supported in part by the National Basic Research Program of China (973 Program) under Grants No. 2010CB833000; the National Nature Science Foundation of China (NSFC) under Grants No. 10905084, No. 11335012 and No. 11475237; The numerical calculations were done using the HPC Cluster of SKLTP/ITP-CAS.

References

1. **PAMELA** Collaboration, O. Adriani et al., *An anomalous positron abundance in cosmic rays with energies 1.5-100 GeV*, *Nature* **458** (2009) 607–609, [[arXiv:0810.4995](#)].
2. O. Adriani, G. Barbarino, G. Bazilevskaya, R. Bellotti, M. Boezio, et al., *A statistical procedure for the identification of positrons in the PAMELA experiment*, *Astropart.Phys.* **34** (2010) 1–11, [[arXiv:1001.3522](#)].
3. **Fermi-LAT** Collaboration, M. Ackermann et al., *Measurement of separate cosmic-ray electron and positron spectra with the Fermi Large Area Telescope*, *Phys.Rev.Lett.* **108** (2012) 011103, [[arXiv:1109.0521](#)].
4. **AMS** Collaboration, L. Accardo et al., *High Statistics Measurement of the Positron Fraction in Primary Cosmic Rays of 0.5C500 GeV with the Alpha Magnetic Spectrometer on the International Space Station*, *Phys.Rev.Lett.* **113** (2014) 121101.

10 Hong-Bo Jin, Yue-Liang Wu and Yu-Feng Zhou

5. J. Kopp, *Constraints on dark matter annihilation from AMS-02 results*, *Phys.Rev.* **D88** (2013) 076013, [arXiv:1304.1184].
6. A. De Simone, A. Riotto, and W. Xue, *Interpretation of AMS-02 Results: Correlations among Dark Matter Signals*, *JCAP* **1305** (2013) 003, [arXiv:1304.1336].
7. I. Cholis and D. Hooper, *Dark Matter and Pulsar Origins of the Rising Cosmic Ray Positron Fraction in Light of New Data From AMS*, *Phys.Rev.* **D88** (2013) 023013, [arXiv:1304.1840].
8. L. Feng, R.-Z. Yang, H.-N. He, T.-K. Dong, Y.-Z. Fan, et al., *AMS-02 positron excess: new bounds on dark matter models and hint for primary electron spectrum hardening*, *Phys.Lett.* **B728** (2014) 250–255, [arXiv:1303.0530].
9. H.-B. Jin, Y.-L. Wu, and Y.-F. Zhou, *Implications of the first AMS-02 measurement for dark matter annihilation and decay*, *JCAP* **1311** (2013) 026, [arXiv:1304.1997].
10. Z.-P. Liu, Y.-L. Wu, and Y.-F. Zhou, *Sommerfeld enhancements with vector, scalar and pseudoscalar force-carriers*, *Phys.Rev.* **D88** (2013) 096008, [arXiv:1305.5438].
11. L. Bergstrom, T. Bringmann, I. Cholis, D. Hooper, and C. Weniger, *New limits on dark matter annihilation from AMS cosmic ray positron data*, *Phys.Rev.Lett.* **111** (2013) 171101, [arXiv:1306.3983].
12. A. Ibarra, A. S. Lamperstorfer, and J. Silk, *Dark matter annihilations and decays after the AMS-02 positron measurements*, *Phys.Rev.* **D89** (2014), no. 6 063539, [arXiv:1309.2570].
13. M. Di Mauro, F. Donato, N. Fornengo, R. Lineros, and A. Vittino, *Interpretation of AMS-02 electrons and positrons data*, *JCAP* **1404** (2014) 006, [arXiv:1402.0321].
14. S.-J. Lin, Q. Yuan, and X.-J. Bi, *Quantitative study of the AMS-02 electron/positron spectra: Implications for pulsars and dark matter properties*, *Phys.Rev.* **D91** (2015), no. 6 063508, [arXiv:1409.6248].
15. M. Ibe, S. Matsumoto, S. Shirai, and T. T. Yanagida, *Mass of Decaying Wino from AMS-02 2014*, *Phys.Lett.* **B741** (2015) 134–137, [arXiv:1409.6920].
16. S.Ting, talk at *AMS-02 days at CERN*, April 15-17, CERN, Geneva, <https://indico.cern.ch/event/381134/timetable/#20150415>.
17. D. Hooper, T. Linden, and P. Mertsch, *What Does The PAMELA Antiproton Spectrum Tell Us About Dark Matter?*, *JCAP* **1503** (2015), no. 03 021, [arXiv:1410.1527].
18. R. Kappl and M. W. Winkler, *The Cosmic Ray Antiproton Background for AMS-02*, *JCAP* **1409** (2014) 051, [arXiv:1408.0299].
19. N. Fornengo, L. Maccione, and A. Vittino, *Constraints on particle dark matter from cosmic-ray antiprotons*, *JCAP* **1404** (2014) 003, [arXiv:1312.3579].
20. M. Cirelli and G. Giesen, *Antiprotons from Dark Matter: Current constraints and future sensitivities*, *JCAP* **1304** (2013) 015, [arXiv:1301.7079].
21. H.-B. Jin, S. Miao, and Y.-F. Zhou, *Implications of the latest XENON100 and cosmic ray antiproton data for isospin violating dark matter*, *Phys.Rev.* **D87** (2013), no. 1 016012, [arXiv:1207.4408].
22. H.-B. Jin, Y.-L. Wu, and Y.-F. Zhou, *Upper limits on DM annihilation cross sections from the first AMS-02 antiproton data*, arXiv:1504.04604.
23. V. Ginzburg, V. Dogiel, V. Berezhinsky, S. Bulanov, and V. Ptuskin, *Astrophysics of cosmic rays*, .
24. A. Strong and I. Moskalenko, *Propagation of cosmic-ray nucleons in the galaxy*, *Astrophys.J.* **509** (1998) 212–228, [astro-ph/9807150].
25. L. Gleeson and W. Axford, *Solar Modulation of Galactic Cosmic Rays*, *Astrophys.J.* **154** (1968) 1011.

26. A. Strong and I. Moskalenko, *Propagation of cosmic-ray nucleons in the galaxy*, *Astrophys.J.* **509** (1998) 212–228, [astro-ph/9807150].
27. I. V. Moskalenko, A. W. Strong, J. F. Ormes, and M. S. Potgieter, *Secondary anti-protons and propagation of cosmic rays in the galaxy and heliosphere*, *Astrophys.J.* **565** (2002) 280–296, [astro-ph/0106567].
28. A. Strong and I. Moskalenko, *Models for galactic cosmic ray propagation*, *Adv.Space Res.* **27** (2001) 717–726, [astro-ph/0101068].
29. I. V. Moskalenko, A. Strong, S. Mashnik, and J. Ormes, *Challenging cosmic ray propagation with antiprotons. Evidence for a fresh nuclei component?*, *Astrophys.J.* **586** (2003) 1050–1066, [astro-ph/0210480].
30. V. Ptuskin, I. V. Moskalenko, F. Jones, A. Strong, and V. Zirakashvili, *Dissipation of magnetohydrodynamic waves on energetic particles: impact on interstellar turbulence and cosmic ray transport*, *Astrophys.J.* **642** (2006) 902–916, [astro-ph/0510335].
31. H.-B. Jin, Y.-L. Wu, and Y.-F. Zhou, *Cosmic ray propagation and dark matter in light of the latest AMS-02 data*, [arXiv:1410.0171](#).
32. F. Donato, N. Fornengo, D. Maurin, and P. Salati, *Antiprotons in cosmic rays from neutralino annihilation*, *Phys.Rev.* **D69** (2004) 063501, [astro-ph/0306207].
33. I. V. Moskalenko, A. W. Strong, J. F. Ormes, and M. S. Potgieter, *Secondary anti-protons and propagation of cosmic rays in the galaxy and heliosphere*, *Astrophys.J.* **565** (2002) 280–296, [astro-ph/0106567].
34. I. V. Moskalenko, A. Strong, S. Mashnik, and J. Ormes, *Challenging cosmic ray propagation with antiprotons. Evidence for a fresh nuclei component?*, *Astrophys.J.* **586** (2003) 1050–1066, [astro-ph/0210480].
35. G. Giesen, M. Boudaud, Y. Genolini, V. Poulin, M. Cirelli, et al., *AMS-02 antiprotons, at last! Secondary astrophysical component and immediate implications for Dark Matter*, [arXiv:1504.04276](#).
36. O. Adriani, G. Barbarino, G. Bazilevskaya, R. Bellotti, M. Boezio, et al., *The PAMELA Mission: Heralding a new era in precision cosmic ray physics*, *Phys.Rept.* **544** (2014) 323–370.
37. T. Sjostrand, S. Mrenna, and P. Z. Skands, *A Brief Introduction to PYTHIA 8.1*, *Comput.Phys.Comm.* **178** (2008) 852–867, [arXiv:0710.3820].
38. J. F. Navarro, C. S. Frenk, and S. D. White, *A Universal density profile from hierarchical clustering*, *Astrophys.J.* **490** (1997) 493–508, [astro-ph/9611107].
39. L. Bergstrom, P. Ullio, and J. H. Buckley, *Observability of gamma-rays from dark matter neutralino annihilations in the Milky Way halo*, *Astropart.Phys.* **9** (1998) 137–162, [astro-ph/9712318].
40. J. Einasto, *Dark Matter*, [arXiv:0901.0632](#).
41. B. Moore, S. Ghigna, F. Governato, G. Lake, T. R. Quinn, et al., *Dark matter substructure within galactic halos*, *Astrophys.J.* **524** (1999) L19–L22, [astro-ph/9907411].
42. J. Diemand, B. Moore, and J. Stadel, *Convergence and scatter of cluster density profiles*, *Mon.Not.Roy.Astron.Soc.* **353** (2004) 624, [astro-ph/0402267].
43. **Fermi-LAT** Collaboration, M. Ackermann et al., *Searching for Dark Matter Annihilation from Milky Way Dwarf Spheroidal Galaxies with Six Years of Fermi-LAT Data*, [arXiv:1503.02641](#).
44. M. Ibe, S. Matsumoto, S. Shirai, and T. T. Yanagida, *Wino Dark Matter in light of the AMS-02 2015 Data*, *Phys. Rev.* **D91** (2015), no. 11 111701, [arXiv:1504.05554].
45. C.-H. Chen, C.-W. Chiang, and T. Nomura, *Dark matter for excess of AMS-02 positrons and antiprotons*, *Phys. Lett.* **B747** (2015) 495–499, [arXiv:1504.07848].